HHS Public Access

Author manuscript

Nat Immunol. Author manuscript; available in PMC 2012 November 01.

Published in final edited form as:

Nat Immunol. 2012 May ; 13(5): 481–490. doi:10.1038/ni.2267.

Ubc13 maintains the suppressive function of regulatory T cells and prevents their conversion into effector-like T cells

Jae-Hoon Chang[1], **Yichuan Xiao**[1], **Hongbo Hu**[1], **Jin Jin**[1], **Jiayi Yu**[1], **Xiaofei Zhou**[1], **Xuefeng Wu**[1,6], **Howard M Johnson**[3], **Shizuo Akira**[4], **Manolis Pasparakis**[5], **Xuhong Cheng**[1], and **Shao-Cong Sun**[1,2]

[1]Department of Immunology, The University of Texas MD Anderson Cancer Center, 7455 Fannin Street, Box 902, Houston TX 77030.

[2]The University of Texas Graduate School of Biomedical Sciences, Houston, TX 77030.

[3]Department of Microbiology and Cell Science, University of Florida, Gainesville, FL 32611.

[4]Laboratory of Host Defense, WPI Immunology Frontier Research Center, Osaka University, 3-1 Yamada-oka, Suita, Osaka 565-0871, Japan.

[5]Institute for Genetics, Center for Molecular Medicine (CMMC), and Cologne Excellence Cluster on Cellular Stress Responses in Aging-Associated Diseases (CECAD), University of Cologne, Cologne, Germany.

Abstract

Maintenance of immune homeostasis requires regulatory T (T_{reg}) cells. Here we show that T_{reg}-specific ablation of Ubc13, a lysine 63-specific ubiquitin-conjugating enzyme, caused aberrant T cell activation and autoimmunity. Although Ubc13 deficiency did not affect T_{reg} cell survival or Foxp3 expression, it impaired the *in vivo* suppressive function of T_{reg} cells and rendered them sensitive for acquiring T helper (T_H) 1- and T_H17-like effector T cell phenotypes. This function of Ubc13 involved its downstream target, IκB kinase (IKK). The Ubc13-IKK signaling axis controlled the expression specific T_{reg} effector molecules, including interleukin 10 (IL-10) and SOCS1. Collectively, these findings suggest that the Ubc13-IKK signaling axis regulates the molecular program that maintains T_{reg} function and prevents T_{reg} cells from acquiring inflammatory phenotypes.

Address correspondence to: Shao-Cong Sun, Department of Immunology, The University of Texas MD Anderson Cancer Center, 7455 Fannin Street, Box 902, Houston TX 77030. Fax: 713-563-3280; Tel: 713-563-3218; ssun@mdanderson.org.

[6]Present address: Laboratory of Gene Regulation and Signal Transduction, Department of Pharmacology, School of Medicine, University of California at San Diego, La Jolla, CA 92093.

AUTHOR CONTRIBUTIONS

J.-H.C. designed and did the research, prepared the figures, and wrote part of the manuscript; Y.X. did the luciferase assays; X.Z. provided technical help in adoptive transfer; H.H. did the Ubc13 IB; J.J. constructed the *Socs1* mut-luc plasmid; J.Y., X.H.C., and X.W. contributed to the generation of mouse models; H.M.J., S.A., and M.P contributed reagents; and S.-C.S. designed the research and wrote the manuscript.

COMPETING FINANCIAL INTERESTS

The authors declare no competing financial interests.

Keywords

Ubc13; ubiquitination; T_{reg}; IKK; NF-κB

Regulatory T (T_{reg}) cells represent a subset of $CD4^+$ T cells with a pivotal role in maintaining peripheral immune tolerance and, thereby, preventing autoimmunity and chronic inflammations[1]. A hallmark of T_{reg} cells is expression of forkhead box P3 (Foxp3), a master transcription factor required for the differentiation, maintenance, and suppressive functions of T_{reg} cells[2]. Foxp3 genetic deficiency causes aberrant activation and homeostasis of T cells, leading to multiorgan inflammation[2]. The suppressive function of T_{reg} cells is mediated through both cell-cell contact and secretion of immunosuppressive cytokines, the latter of which include transforming growth factor-β (TGF-β), interleukin 10 (IL-10) and IL-35[1,3].

T_{reg} cells are generally stable; however, a fraction of them may lose Foxp3 expression and undergo phenotypic changes to acquire diverse effector functions under lymphopenic and/or inflammatory conditions[4–6]. Studies using different *in vivo* models have demonstrated the conversion of T_{reg} cells into T_H1-, T_H17-, or T_{FH}-like effector T cells, which appears to contribute to uncontrolled chronic inflammation and autoimmunity[7–10]. The acquisition of inflammatory effector functions by T_{reg} cells may even occur without losing Foxp3 expression[7,11–13]. Although the mechanisms mediating the phenotypic conversion of T_{reg} cells are still poorly understood, proinflammatory cytokines were shown to play a role[7,14]. Moreover, the stability and suppressive function of T_{reg} cells rely on expression of SOCS1 (suppressor of cytokine signaling 1), a molecule that negatively regulates the signaling function of several cytokine receptors[13,15]. SOCS1 inhibits the activation of both STAT1 and STAT3, thereby restraining T_{reg} cells from being converting into T_H1- and T_H17-like effector T cells[13].

The T cell receptors (TCRs) of T_{reg} cells recognize both self and non-self antigens and appear to be constantly stimulated *in vivo*[16]. However, how the TCR-mediated signaling pathways regulate the stability and suppressive function of T_{reg} cells remains poorly understood. One major TCR-elicited pathway involves activation of a signaling complex composed of Carma1, Bcl-10, Molt1, and the E2 ubiquitin-conjugating enzyme Ubc13[17]. Although mammalian cells express multiple E2 ubiquitin-conjugating enzymes, Ubc13 is unique in that it specifically conjugates lysine 63 (K63)-linked polyubiquitin chains known to be critical for activation of IκB kinase (IKK) and its downstream transcription factor NF-κB[17]. Thus, a major function of Ubc13 in conventional T cells is to mediate TCR-stimulated IKK-NF-κB activation and peripheral T cell homeostasis[18,19]. Recent studies have demonstrated an important role for the NF-κB family member c-Rel in the regulation of T_{reg} cell differentiation[20–23]; however, whether the Ubc13-IKK-regulated signaling pathway has a role in regulating the homeostasis, stability, or suppressive function of committed T_{reg} cells is unknown.

Here we studied the role of Ubc13 by conditional ablation of the Ubc13-coding gene *Ube2n*. We found that Ubc13 is dispensable for the survival and homeostasis of T_{reg} cells as well as their *in vitro* suppressive activity. Ubc13 however had a pivotal role in maintaining the *in*

vivo immunosuppressive function of T_{reg} cells and in preventing the conversion of T_{reg} cells into T_H1- and T_H17-like effector T cells in a manner dependent on its downstream target IKK. The Ubc13-IKK signaling axis is dispensable for expression of T_{reg} signature genes but is required for expression of specific T_{reg} functional factors, including IL-10 and SOCS1. These findings suggest that the Ubc13-IKK signaling axis is an important part of the signaling program that maintains the stability and immunosuppressive function of T_{reg} cells.

RESULTS

Multiorgan inflammation by T_{reg}-specific ablation of Ubc13

To examine the T_{reg}-specific function of Ubc13, we generated T_{reg}-specific conditional *Ube2n*-deficient mice by crossing *Ube2n*-floxed (*Ube2n*$^{fl/fl}$) mice[24] with the Foxp3-GFP-hCre mice[25]. The resulting *Ube2n*$^{fl/fl}$Foxp3$^{GFP\text{-}hCre}$ (hereafter called *Ube2n*$^{Treg\text{-}KO}$) mice and their age-matched *Ube2n*$^{+/+}$Foxp3$^{GFP\text{-}hCre}$ wild-type controls were used for experiments. Specific deletion of Ubc13 in T_{reg}, but not in CD4$^+$ conventional T cells, was confirmed by Ubc13 immunoblotting (Fig. 1a). *Ube2n*$^{Treg\text{-}KO}$ mice were born at expected Mendelian ratios and appeared to be grossly normal at young ages. However, starting from 8 weeks of age, they displayed weight reduction compared to the age-matched wild-type controls, a phenotype that became more prominent at 12 weeks of age or older (Fig. 1b). This phenotype of the *Ube2n*$^{Treg\text{-}KO}$ mice was associated with autoimmune symptoms, including increased size and cellularity of peripheral lymphoid organs (Fig. 1c and data not shown) and lymphocytic infiltration into multiple nonlymphoid organs (Fig. 1d). These pathological phenotypes were reminiscent of those reported in T_{reg}-deficient mice[2]. However, in general, the disease severity in *Ube2n*$^{Treg\text{-}KO}$ mice was milder than that of T_{reg}-deficient mice and was not associated with fatality. These findings suggest that Ubc13 may regulate certain aspects of the T_{reg} cell function.

Abnormal conventional T cell activation in *Ube2n*$^{Treg\text{-}KO}$ mice

An important function of T_{reg} cells is to prevent abnormal T cell activation and maintain immune cell homeostasis. We found that the percentage of CD4$^+$ and CD8$^+$ T cells was lower in the spleen and lymph nodes (LNs) of the *Ube2n*$^{Treg\text{-}KO}$ mice (Supplementary Fig. 1a). However, this was not due to a reduction in the number of T cells (Supplementary Fig. 1b) but apparently resulted from an increase in the population of non-T cells (CD4$^-$CD8$^-$) associated with the splenomegaly and lymphadenopsy (Supplementary Fig. 1a). This abnormality was not detected in younger mice (4 week old) that had no autoimmune phenotypes (Supplementary Fig. 1c, d). The non-T cell population in the older *Ube2n*$^{Treg\text{-}KO}$ mice included predominantly B220$^+$ B cells in the mesenteric LNs (MLNs) (Supplementary Fig. 2a), but also B220$^-$CD3$^-$ cells, such as CD11c$^+$ and F4/80$^+$ myeloid cells and NK1.1$^+$ NK cells, in the spleen (Supplementary Fig. 2b). To look at T cell homeostasis in *Ube2n*$^{Treg\text{-}KO}$ mice, we quantified the memory and naïve (Ubc13-sufficient) T cells based on surface expression of CD44 and CD62L. In both the spleen and LNs, the *Ube2n*$^{Treg\text{-}KO}$ mice had a significant increase in the frequency of memory and effector-like (CD44^{hi}CD62L^{lo}) CD4$^+$ T cells with concomitant reduction in the frequency of naïve (CD44^{lo}CD62L^{hi}) CD4$^+$ T cells (Fig. 2a,b). The absolute number of memory and effector-

like CD4+ T cells was also significantly increased in the *Ube2n*$^{Treg\text{-}KO}$ mice (Fig. 2c). Consistent with these findings, the *Ube2n*$^{Treg\text{-}KO}$ mice had a significantly increased frequency of T_H1, T_H2, and T_H17 CD4+ effector T cells in the spleen (Fig. 2d).

Because the intestine is an organ that is often affected by impaired T_{reg} cell function, we examined the effect of T_{reg}-specific Ubc13 ablation on the frequency of T cells in the lamina propria of this organ. Indeed, the lamina propria of both the small and the large intestines of *Ube2n*$^{Treg\text{-}KO}$ mice had a marked increase in the frequency of CD4+ and CD8+ T cells (Fig. 2e). Within the CD4+ T cell population, there was a significant increase in the frequency of T_H17 cells (Fig. 2f). The large intestine, although not the small intestine, also had a moderate increase in T_H1 cell frequency (Fig. 2f). Thus, loss of Ubc13 in T_{reg} cells impaired the homeostasis of the Ubc13-sufficient conventional T cells, which further indicates a role for Ubc13 in regulating the immunosuppressive function of T_{reg} cells.

Ubc13 is dispensable for T_{reg} survival or *in vitro* function

Wild-type and *Ube2n*$^{Treg\text{-}KO}$ mice contained comparable frequency of Foxp3+ T_{reg} cells in both the thymus and the peripheral lymphoid organs (Supplementary Fig. 3a,b), suggesting that Ubc13 is dispensable for T_{reg} homeostasis. To further confirm this conclusion, we used Rosa26-YFP Cre reporter (hereafter called R26^{YFP}) mice that express YFP in a Cre-dependent manner[26]. The progeny of R26^{YFP} mice crossed with Foxp3^{Cre} mice express YFP specifically in T_{reg} cells[25]. Because GFP is less bright compared to YFP (Supplementary Fig. 4), so GFP should not interfere with the YFP signal during analysis, and because all GFP+ cells were YFP+ (Supplementary Fig. 4), we used either YFP or Foxp3 as a marker for T_{reg} cells in our subsequent analyses. As seen in the Foxp3 staining experiments, young R26^{YFP} and *Ube2n*$^{Treg\text{-}KO}$R26^{YFP} mice had comparable YFP+ T_{reg} frequencies (Fig. 3a,b) and numbers (Fig. 3c) in all of the immune organs analyzed. At an older age (10 week), *Ube2n*$^{Treg\text{-}KO}$R26^{YFP} mice had a reduced T_{reg} percentage in the spleen (Fig. 3b), which was not due to the reduction in T_{reg} numbers (Fig. 3c) but was apparently caused by the uncontrolled expansion of the Ubc13-sufficient conventional T cells (Fig. 3d).

I*n vitro* T_{reg} assays revealed that the wild-type and Ubc13-deficient T_{reg} cells displayed comparable ability to suppress the activation of CD4+ naïve T cells (Fig. 3e). Thus, unlike Foxp3 deficiency, the loss of Ubc13 did not compromise the overall suppressive capacity of T_{reg} cells.

Ubc13 is required for T_{reg} function *in vivo*

To examine the *in vivo* function of T_{reg} cells, we employed a well-characterized adoptive transfer approach[27]. Transfer of CD45RB^{hi} naïve CD4+ T cells to *Rag1*$^{-/-}$ mice induced overt autoimmunity, defined by gradual weight loss (Fig. 4a), splenomegaly and lymphadenopasy (Fig. 4b), increased frequency of memory and effector-like T cells (Fig. 4c) and hyperplasia of the colonic mucosa (Fig. 4d). Co-transfer of wild-type T_{reg} cells, but not Ubc13-deficient T_{reg} cells, effectively suppressed the autoimmune phenotypes of the naïve CD4+ T cells (Fig. 4a-d), suggesting a marked attenuation of the suppressive activity of Ubc13-deficient T_{reg} cells. Thus, although Ubc13 is dispensable for the homeostasis and

in vitro activity of T_{reg} cells, Ubc13 is required for the immunosuppressive function of T_{reg} cells *in vivo*, a finding that explains the autoimmune phenotype of the *Ube2n*$^{Treg\text{-}KO}$ mice.

When T_{reg} cells were transferred in the absence of CD45RB^{hi} naïve CD4$^+$ T cells, they did not induce severe loss of bodyweight; however, in contrast to recipients of wild-type T_{reg} cells, the recipients of Ubc13-deficient T_{reg} cells failed to gain weight during the 5-week post-transfer period, indicative of a disease phenotype (Fig. 4e), had splenomegaly coupled with increased spleen cellularity (Fig. 4f,g) as well as a markedly higher number of transferred T_{reg} cells, suggesting their abnormal expansion (Fig. 4h). Abnormal expansion of Ubc13-deficient T_{reg} cells was also detected when they were cotransferred with CD45RB^{hi} naïve CD4$^+$ T cells (Supplementary Fig. 5a). Since the Ubc13-deficient T_{reg} cells displayed only a moderate reduction in apoptosis (Supplementary Fig. 5b), transferred Ubc13-deficient T_{reg} cells might possess increased expansion ability. We found that the pathological phenotypes of Ubc13-deficient T_{reg} cells were efficiently suppressed when they were cotransferred with wild-type T_{reg} cells (Fig. 4e–h). Collectively, these results indicate that the Ubc13-deficient T_{reg} cells may acquire certain inflammatory functions under lymphopenic conditions that can be controlled by wild-type T_{reg} cells.

Effector function acquistion by Ubc13-deficient T_{reg} cells

Recent studies suggest that T_{reg} cells may acquire the pathological ability to produce proinflammatory cytokines when functionally perturbed by genetic alterations or environmental conditions[5, 6, 13]. Because of the pathological phenotype of the Ubc13-deficient T_{reg} cells, we asked whether Ubc13 had a role in maintaining the stability of T_{reg} cells under lymphopenic or inflammatory conditions. YFP$^+$ T_{reg} cells purified from young (6 week) R26^{YFP} and *Ube2n*$^{Treg\text{-}KO}$R26^{YFP} mice were almost exclusively Foxp3$^+$, suggesting stable Foxp3 expression (Supplementary Fig. 6a). In agreement with previous studies[5,6,10], when YFP$^+$ T_{reg} cells were adoptively transferred into Rag1-deficient mice together with wild-type CD45RB^{hi} naïve CD4$^+$ T cells, a fraction of the T_{reg} cells lost Foxp3, and this happened at comparable levels in Ubc13-sufficient and the Ubc13-deficient T_{reg} cells (Supplementary Fig. 6b).

Because T_{reg} cell conversion into effector-like T cells often occurs without losing Foxp3 expression[7,11–13], we next examined the possible acquisition of effector functions in the transferred T_{reg} cells in the MLNs. Consistent with the idea that the majority of T_{reg} cells are stable[6], only a small fraction of the Ubc13-sufficient T_{reg} cells acquired the ability to produce interferon-γ (IFN-γ) and IL-17 10 and 21 days after transfer (Fig. 5a). However, a substantially higher frequency of Ubc13-deficient T_{reg} cells displayed a T_H1- and T_H17-like effector phenotype (Fig. 5a,b). Some of the converted Ubc13-deficient T_{reg} cells were IFN-γ-IL-17 double positive.

We next examined whether the effector phenotype acquisition by the Ubc13-deficient T_{reg} cells depended on the cotransferred naïve CD4$^+$ T cells. Interestingly, even when transferred alone, Ubc13-deficient T_{reg} cells acquired effector T cell phenotype (Fig. 5c), with a large proportion of these mutant T_{reg} cells displaying an IFN-γ$^+$ T_H1-like effector phenotype, although the frequency of IL-17$^+$ and IL-17$^+$IFN-γ$^+$ cells was also increased compared to wild-type T_{reg} cells (Fig. 5c). The effector T cell phenotype of Ubc13-deficient T_{reg} cells

was not suppressed by the cotransfer of wild-type T_{reg} cells. Instead, wild-type T_{reg} cells promoted the shift of Ubc13-deficient T_{reg} cells from an IFN-γ^+ to an IL-17^+ and IL-17^+IFN-γ^+ effector phenotype (Fig. 5c). We also analyzed Foxp3 expression in the transferred T_{reg} cells. Consistent with a recent study[13], we found that in the absence of naïve T cells, transferred T_{reg} cells had a profound loss of Foxp3. This was similarly seen in wild-type T_{reg} and Ubc13-deficient T_{reg} cells (Fig. 5d).

We next examined whether Ubc13-deficient T_{reg} cells acquired an effector phenotypes under non-transfer conditions, in *Ube2n*$^{Treg\text{-}KO}$ mice, at the time of overt autoimmune symptoms (Fig. 5e). Gating on either Foxp3^+ (T_{reg}) or YFP^+ (T_{reg} and ex-Foxp3) cells, we detected a fraction of T_{reg} cells expressing IFN-γ or IL-17 in the *Ube2n*$^{Treg\text{-}KO}$R26^{YFP}, but not the R26^{YFP} mice (Fig. 5e). Consistently, ELISA revealed that the Ubc13-deficient T_{reg} cells secreted significantly more IFN-γ and IL-17 than wild-type T_{reg} cells (Fig. 5f). Thus, Ubc13 maintains the integrity of T_{reg} cells at steady-state.

T_{reg} conversion into T_H17-like cells can be induced *in vitro* by the proinflammatory cytokine IL-6 or by IL-6 in combination with other cytokines[7,14]. We found that YFP^+ T_{reg} cells purified from 6 week old R26^{YFP} and *Ube2n*$^{Treg\text{-}KO}$R26^{YFP} mice were largely inert in the production of effector cytokines (data not shown). Furthermore, *ex vivo* activation of purified T_{reg} cells under neutral conditions led to the induction of a small percentage of IL-17-producing cells, which was not substantially different between the control and Ubc13-deficient T_{reg} cells (Fig. 5g). However, upon activation in the presence of IL-6 and TGF-β, Ubc13-deficient T_{reg} cells produced a substantially higher percentage of T_H17-like cells than wild-type T_{reg} cells (Fig. 5g,h). Acquisition of an effector T cell phenotype was not associated with loss of Foxp3. Collectively, these results suggest that Ubc13 deficiency rendered T_{reg} cells sensitive to acquiring T_H1- and T_H17-like effector activity under lymphopenic and inflammatory conditions.

IKK mediates the function of Ubc13 in T_{reg} cells

A major signaling function of Ubc13 in T cells is to mediate TCR-CD28-stimulated activation of IKK-NF-κB signaling pathway[18,19]. Consistently, we found that crosslinking of TCR and CD28 in wild-type, but not in Ubc13-deficient, T_{reg} cells induced the phosphorylation of RelA (Fig. 6a), a molecular event known to be mediated by IKK2 (also called IKKβ)[28]. To examine whether impaired IKK-NF-κB signaling is responsible for the immunosuppressive defect of Ubc13-deficient T_{reg} cells, we rescued this pathway by employing a transgenic mouse carrying a constitutively active *IKK2* (*IKK2CA*) transgene under the control of a loxP-flanked Stop cassette. In this transgenic system, the expression of IKK2CA occurs conditionally when crossed with cell-specific Cre mice[29]. By crossing this *IKK2CA*-floxed transgenic (Tg) mouse with the *Ube2n*$^{f/f}$Foxp3$^{GFP\text{-}Cre}$ mice, we generated age-matched *Ube2n*$^{+/+}$*IKK2CA*$^{Tg/+}$Foxp3$^{GFP\text{-}Cre}$ (hereafter named WT-*IKK2CA*$^{Treg\text{-}Tg}$) and *Ube2n*$^{fl/fl}$*IKK2CA*$^{Tg/+}$Foxp3$^{GFP\text{-}Cre}$ (hereafter named *Ube2n*$^{Treg\text{-}KO}$*IKK2CA*$^{Treg\text{-}Tg}$) mice.

T_{reg}-specific expression of the *IKK2CA* transgene, in either WT or *Ube2n*$^{Treg\text{-}KO}$ background, did not substantially alter the homeostasis of T_{reg} cells (Supplementary Fig. 7). However, IKK2CA rescued the suppressive function of Ubc13-deficient T_{reg} cells, as

indicated by the reduction of memory and effector-like CD4$^+$ T cell in *Ube2n*$^{\text{Treg-KO}}$*IKK2CA*$^{\text{Treg-Tg}}$ mice (Fig. 6b). T_{reg}-specific expression of IKK2CA did not appreciably alter the frequency of memory-effector-like T cells in wild-type mice (Fig. 6b). To examine whether IKK2 was required for T_{reg} function, we generated T_{reg}-conditional IKK2-deficient mice by crossing *IKK2*-floxed mice[30] with the Foxp3-GFP-hCre mice[25], resulting in *IKK2*$^{\text{fl/fl}}$Foxp3$^{\text{GFP-hCre}}$ (hereafter called *IKK2*$^{\text{Treg-KO}}$) and age-matched *IKK2*$^{+/+}$Foxp3$^{\text{GFP-hCre}}$ littermate control (hereafter called wild-type) mice. As seen in *Ube2n*$^{\text{Treg-KO}}$ mice, *IKK2*$^{\text{Treg-KO}}$ mice had a marked increase in the frequency (Fig. 6c, d) and number (Fig. 6e) of memory and effector-like T cells in peripheral lymphoid organs. Furthermore, the frequency of effector CD4$^+$ T cells producing IL-17 and IFN-γ was greatly increased (Supplementary Fig. 8a,b). However, like in the case of Ubc13 deficiency (Fig. 3a-d), the loss of IKK2 in T_{reg} cells did not substantially alter T_{reg} homeostasis (Supplementary Fig. 9a). The moderate reduction in the frequency of T_{reg} cells observed in *IKK2*$^{\text{Treg-KO}}$ mice might be due to the expansion of IKK2-sufficient effector T cells, because the absolute number of T_{reg} cells was comparable in IKK2-deficient and wild-type mice (Supplementary Fig. 9b). Moreover, the IKK2-deficient T_{reg} cells resembled the Ubc13-deficient T_{reg} cells in that they were vulnerable to acquisition of T_H17- and T_H1-like effector functions *in vivo* (Supplementary Fig. 10a,b). These findings suggest an important role for the Ubc13-IKK signaling axis in maintaining the function and stability of T_{reg} cells.

Ubc13 regulates T_{reg} expression of SOCS1 and IL-10

To further explore the molecular mechanism by which Ubc13 regulates the function of T_{reg} cells, we examined the effect of T_{reg}-specific Ubc13 deletion on the expression of various T_{reg} signature genes. Ubc13 deficiency did not inhibit the expression of a panel of well-characterized T_{reg} markers in young mice (5 weeks old) (Fig. 7a). In older (8 weeks) *Ube2n*$^{\text{Treg-KO}}$ mice, T_{reg} cells displayed moderately increased expression of several T_{reg} markers, including ICOS, OX40, CTLA-4, and GITR (data not shown), probably due to the inflammatory environment in these mice. Because Foxp3 is largely responsible for the expression of these T_{reg} markers, this result was consistent with the dispensable role of Ubc13 in the expression of Foxp3.

We next performed real-time RT-PCR to measure the expression of various cytokine genes involved in the suppressive function and effector conversion of T_{reg} cells. The Ubc13-deficient T_{reg} cells competently expressed *Tgfb1*; however, the expression of *Il10* was attenuated (Fig. 7b). This result was further confirmed by flow cytometry (Fig. 7c) and ELISA (Fig. 7d). The IL-10 expression defect of Ubc13-deficient T_{reg} cells was largely rescued by expression of the *IKK2CA* transgene, suggesting the involvement of IKK signaling axis (Supplementary Fig. 11). Because the IL-10 receptor signaling plays an important role in T_{reg} function, particularly in the control of T_H17-cell responses[31–33], this finding partially explains the functional impairment of Ubc13-deficient T_{reg} cells.

Another gene that was substantially affected by Ubc13 deficiency was *Socs1* (Fig. 7b), which is known to regulate T_{reg} stability and prevent T_{reg} conversion into T_H1- and T_H17-like effector T cells[13]. SOCS1, as well as its homologue SOCS3, negatively regulate signal transduction stimulated by different cytokines, including IL-6, which stimulates T_{reg}

conversion. Consistent with a prior report[34], SOCS3 expression was extremely low in both control and Ubc13-deficient T_{reg} cells (data not shown), while SOCS1 was abundantly expression in the wild-type but not in Ubc13-deficient T_{reg} cells (Fig. 7b). Flow cytometry also showed strong expression of SOCS1 protein in wild-type T_{reg} cells and substantially reduced expression in Ubc13-deficient T_{reg} cells (Fig. 7e). Furthermore, the expression of *Il10* and *Socs1* was also reduced in IKK2-deficient T_{reg} cells (Supplementary Fig. 12).

The *Il10* promoter is known to contain functional binding sites for NF-κB and STAT[35,36], while the role of NF-κB in *Socs1* gene regulation is less well defined. The *Socs1* promoter contains STAT-binding sites and responds to stimulation by IFN-γ and IL-6[37]. However, optimal induction of SOCS1 in T cells requires the synergy of cytokine and TCR signals[38]. SOCS1 is also induced by human T-cell leukemia virus type I, which appears to involve IKK-NF-κB activation[39]. To examine the role of the IKK-NF-κB pathway in SOCS1 expression, we tested if the T_{reg}-specific *IKK2CA* transgene can rescue SOCS1 expression in Ubc13-deficient T_{reg} cells. SOCS1 expression was largely rescued in T_{reg} cells from *Ube2n*$^{\text{Treg-KO}}$*IKK2CA*$^{\text{Treg-Tg}}$ (Fig. 7f,). By analyzing the conserved noncoding sequences of the *Socs1* gene, we identified a putative NF-κB-binding site that is highly conserved among different species and overlaps with a previously identified STAT-binding site to form a putative STAT-NF-κB composite (Fig. 8a). In luciferase reporter assays, a wild-type *Socs1* promoter was activated by TCR-CD28 stimuli in synergy with IFN-γ or IL-6, while activation of a STAT-NF-κB binding site mutant *Socs1* promoter was impaired (Fig. 8b). In similar reporter assays, a constitutive form of *STAT3* (*STAT3C*) synergized with *IKK2CA* to activate the *Socs1* promoter, in a manner dependent on the STAT-NF-κB composite site as well (Fig. 8c). These findings emphasize an important role for the Ubc13-IKK axis in maintaining expression of IL-10 and SOCS1 in T_{reg} cells and suggest the direct involvement of NF-κB in mediating *Socs1* gene induction.

SOCS1 plays a role in modulating T_{reg} stability

To determine whether the reduced SOCS1 expression in Ubc13-deficient T_{reg} cells contributed to their functional abnormality, we used a SOCS1 mimetic peptide that spans the kinase inhibitory region (KIR) of SOCS1 and is known to effectively inhibit IL-6 and IFN-γ signaling *in vitro* and partially rescue SOCS1 function *in vivo*[15,40–42]. SOCS1-KIR peptide, but not the control peptide SOCS1-KIR2A, significantly inhibited the conversion of Ubc13-deficient T_{reg} cells to T_H17-like cells *in vitro* (Fig. 9a). At the dose used, SOCS1-KIR did not significantly inhibit the conversion of wild-type T_{reg} cells, probably due to the already high levels of endogenous SOCS1.

We next examined whether SOCS1-KIR could rescue the functional defect of Ubc13-deficient T_{reg} cells *in vivo* using the CD45RB^{hi} T-cell transfer model. The *Rag1* KO mice adoptively transferred with CD45RB^{hi} naïve CD4$^+$ T cells plus Ubc13-deficient T_{reg} cells experienced severe weight loss (Fig. 9b). Repeated injection of SOCS1-KIR, but not the control SOCS1-KIR2A, into these recipient mice substantially, although not completely, prevented their weight loss (Fig. 9b). Furthermore, injection of SOCS1-KIR, but not SOCS1-KIR2A, also partially inhibited the conversion of Ubc13-deficient T_{reg} cells into inflammatory effector T cells *in vivo* (Fig. 9c). Although direct suppression of effector T

cells may account for the *in vivo* effect of SOCS1-KIR treatment, these results indicate a role for Ubc13-mediated SOCS1 expression in the maintenance of T_{reg} stability.

DISCUSSION

Here we identify the ubiquitin-conjugating enzyme (E2) Ubc13 as a mediator of T_{reg}-intrinsic function in immune tolerance. Because Ubc13 is the predominant E2 that conjugates K63-linked ubiquitin chains, this finding further emphasizes a role for K63 ubiquitination in T_{reg} function. We found that T_{reg}-specific ablation of Ubc13 impaired the *in vivo* immunosuppressive function of T_{reg} cells, causing aberrant activation and homeostasis of conventional T cells and multiorgan inflammation. Unlike most other known T_{reg} regulators, Ubc13 was dispensable for maintaining the expression of Foxp3 and various T_{reg} signature genes. Consistently, the autoimmune disease of the *Ube2n*$^{Treg\text{-}KO}$ mice was relatively milder than that of the Scurfy mice or Foxp3-deficient mice that completely lack T_{reg} cells[2]. This phenotype suggests that Ubc13 regulates specific aspects of T_{reg} functions, rather than controls the overall suppressive activity of T_{reg} cells.

Our data suggest that Ubc13 has an important role in preventing the conversion of T_{reg} cells into T_H1- and T_H17-like effector T cells under lymphopenic conditions. Transfer of T_{reg} cells into Rag1-deficient mice, either alone or along with CD45RB^{hi} naïve CD4$^+$ T cells, induced a large portion of the Ubc13-deficient T_{reg} cells to acquire the ability to produce the proinflammatory cytokines IL-17 and IFN-γ, in contrast to only a small fraction of transferred wild-type cells. Moreover, the acquisition of effector-like functions by Ubc13-deficient T_{reg} cells occurred without losing the expression of Foxp3, thus distinguishing Ubc13 from the known Foxp3-regulatory factors. We believe that the Ubc13 signaling pathway maintains T_{reg} stability by reducing the sensitivity of T_{reg} cells to environmental factors. Under inflammatory conditions, a fraction of Foxp3$^+$ T_{reg} cells can simultaneously express effector T cell cytokines, particularly IL-17[7,11,12,43]. These findings suggest that proinflammatory cytokines may partially override the inhibitory function of Foxp3. In support of this idea, we found that activation of T_{reg} cells *in vitro* in the presence of IL-6 and TGF-β induces the production of Foxp3$^+$IL-17$^+$ T cells. Thus, Ubc13-deficient T_{reg} cells were more sensitive to cytokine-induced conversion *in vitro*.

A major downstream signaling molecule of Ubc13 is IKK[17–19]. It is possible that MAP kinases, known to be regulated by Ubc13[19], also play a role, but both gain-of-function and loss-of-function studies suggest an important role of the IKK pathway downstream Ubc13. Although previous studies suggest a role for IKK-NF-κB in regulating Foxp3 expression and T_{reg} development, they did not address the role of IKK-NF-κB in regulating the stability and functionality of committed T_{reg} cells[20–23]. Our data suggest that the Ubc13-IKK signaling axis induces specific genes involved in the regulation of T_{reg} stability and function. We have identified *Il10* and *Socs1* as two important genes regulated by this pathway.

Our findings suggest *Socs1* to be a direct target gene of the Ubc13-IKK signaling axis that is synergistically transactivated by STAT and NF-κB in T_{reg} cells. Strong evidence suggests that *Il10* may also be a gene that is cooperatively regulated by STAT and NF-κB. A prior

study has identified an NF-κB-binding sequence (−54 TGCCAGGAAGGCCCC −43) in the murine *Il10* promoter[35]. We noticed that this NF-κB site is overlapping with a previously identified STAT-binding site (−54 TGCCAGGAA −46)[36]. These studies suggest the involvement of both NF-κB and STAT3 in the induction of *Il10* gene expression, although it remains to be examined whether this putative STAT-NF-κB composite is required for *Il10* induction by TCR-CD28 or TCR-CD28 in combination with cytokines[35, 36]. Given the important role of T_{reg}-derived IL-10 in mediating the *in vivo* function of T_{reg} cells, especially in the suppression of T_H17 cells[31,33], the reduced IL-10 expression may contribute to the impaired *in vivo* function of Ubc13-deficient T_{reg} cells. Future studies need to address whether the Ubc13-IKK signaling pathway mediates expression of additional genes involved in the stability and function of T_{reg} cells.

In conclusion, we present genetic evidence for the involvement of Ubc13-IKK signaling axis in the control of T_{reg} cell stability and function. We propose that Ubc13-IKK regulates the expression of specific molecules involved in the suppressive function and phenotypic stabilization of T_{reg} cells. These findings provide novel insight into the signaling mechanisms that mediate T_{reg} function and also suggest Ubc13 as a possible therapeutic target for the pharmacological manipulation of T_{reg} function.

METHODS

Mice

IKK2-floxed and *Ube2n*-floxed mice were as described[24, 30]. Foxp3-GFP-hCre BAC transgenic mice[25] (Jackson Lab) were backcrossed for 9 generations to the C57BL/6 background and then crossed with *Ube2n*-floxed mice to produce age-matched *Ube2n*$^{+/+}$Foxp3$^{GFP\text{-}hCre}$ (termed WT) and *Ube2n*$^{fl/fl}$Foxp3 $^{GFP\text{-}hCre}$ (termed *Ube2n*$^{Treg\text{-}KO}$) mice. The WT and *IKK2*$^{Treg\text{-}KO}$ mice were similarly generated. In some experiments, these mice were further crossed with the Rosa26-YFP Cre reporter (termed R26^{YFP})[26] (Jackson Lab) to generate WT and *Ube2n*$^{Treg\text{-}KO}$ mice that express YFP in their T_{reg} cells (termed WT-R26^{YFP} and *Ube2n*$^{Treg\text{-}KO}$R26^{YFP} mice, respectively). *IKK2CA* transgenic mice (*IKK2CA*^{Tg}; Jackson Lab) carry a constitutively active *IKK2* (*IKK2CA*) transgene under the control of a loxP-flanked stop cassette[29]. These mice were crossed with the Foxp3-GFP-hCre mice to generate *IKK2CA*$^{Tg/+}$Foxp3 $^{GFP\text{-}hCre}$ (termed *IKK2CA*$^{Treg\text{-}Tg}$) mice. These mice were further crossed with the *Ube2n*$^{Treg\text{-}KO}$ mice to generate age-matched *Ube2n*$^{+/+}$*IKK2CA*$^{Tg/+}$Foxp3-GFP-hCre (WT-*IKK2CA*$^{Treg\text{-}Tg}$), and *Ube2n*$^{fl/fl}$*IKK2CA*$^{Tg/+}$ Foxp3-GFP-hCre (*Ube2n*$^{Treg\text{-}KO}$*IKK2CA*$^{Treg\text{-}Tg}$) mice. B6.SJL mice expressing the CD45.1 congenic marker and *Rag1* KO mice (B6 background) were from Jackson Lab. Mice were maintained in specific pathogen-free facility of The University of Texas MD Anderson Cancer Center, and all animal experiments were in accordance with protocols approved by the Institutional Animal Care and Use Committee of the University of Texas MD Anderson Cancer Center.

Plasmids, antibodies, and reagents

The expression vectors encoding a FLAG-tagged active *STAT3* (*STAT3-C* Flag pRc-CMV) and an HA-tagged active *IKK*β (S177,181E; named *IKK2CA* in this study) were from

Addgene and Dr. Michael Karin, respectively. RelA vector was described previously[44]. *Socs1*-luc (previously named pSI2) is a firefly luciferase reporter driven by an 835-base pair murine *Socs1* promoter[37] (provided by Dr. Tadamitsu Kishimoto). *Socs1* mut-luc was created by site-directed mutagenesis to substitute three nucleotides (GAA to CCG) in the STAT-NF-κB composite of the *Socs1*-luc (see Fig. 8a).

Agonistic anti-CD3 and anti-CD28 antibodies were from eBioscience, anti-UBC13 (Zymed) anti-Hsp60 (H-1) were from Santa Cruz, and other antibodies are listed in the section of flow cytometric analysis. The SOCS1 mimetic peptide SOCS1-KIR and its negative control SOCS1-KIR2A were as described previously[42]. PMA (phorbol 12-myristate 13-acetate) and ionomycin were from Sigma; IL-6, TGF-β, and IFN-γ were from PeproTech.

Cell isolation from intestinal lamina propria

Intestines were treated twice with PBS containing 10% FBS, 20 mM HEPES, 100 U/ml penicillin, 100 μg/ml streptomycin, and 10 mM EDTA for 20 min at 37°C, to remove epithelial cells, and then digested with 400 Mandl U/ml collagenase D (Roche Applied Science) and 50 μg/ml DNase I (Sigma-Aldrich), to isolate mononuclear cells from the lamina propria. Cells were then enriched by a discontinuous density gradient containing 40 and 75% Percoll (Amersham Bioscience).

Flow cytometric analysis

Flow cytometric analyses and cell sorting were performed[45] using a FACSCalibur (BD Bioscience) and FACSAria (BD bioscience), respectively. For RelA phospho-flow, sorted YFP^+CD4^+ T_{reg} cells were preincubated on ice with anti-CD3 plus anti-CD28 and then stimulated at 37°C by crosslinking using an anti-immunoglobulin antibody[45]. Cells were stained with the phospho-NF-κB p65(Ser536) antibody. For intracellular cytokine staining (ICS), cells were stimulated with PMA (50 ng/ml) plus ionomycine (750 ng/ml) for 4–6 hrs in the presence of monensin (10 μg/ml), and the fixed cells were incubated with the indicated antibodies and subjected to flow cytometry. Fluorescence-labeled antibodies used include phycoerythrin (PE)-conjugated anti-IL-17, anti-IL-10, anti-CD8, anti-CD25, anti-CD127, anti-CD137, anti-ICOS (eBioscience); FITC-conjugated anti-Foxp3 (eBioscience) and anti-CD62L (BD Bioscience); APC-conjugated anti-Foxp3, anti-CD44, anti-IFN-γ and anti-CD4 (eBioscience); PE-conjugated anti-CD103, anti-CD122, anti-CD126, anti-OX40, anti-GITR (BD Bioscience); Biotin-conjugated anti-SOCS1 (MBL); anti-phospho-NF-κB p65(Ser536) and APC-conjugated anti-Rabbit IgG (Cell Signaling).

In vitro T_{reg} suppression assay

CFSE-labeled naïve $CD4^+CD25^-$ T cells (1×10^5) were co-cultured with an increasing ratio of sorted T_{reg} cells in the presence of anti-CD3 (1μg/ml) plus irradiated T-cell-depleted spenocytes (5×10^4) in 96-well plates for 4 days. The suppressive function of T_{reg} cells was determined by measuring the proliferation of activated CD4 effector T cells based on CFSE dilution[45].

In vitro T_{reg} conversion assay

Purified YFP$^+$ T_{reg} cells from WT and *Ube2n*$^{Treg\text{-}KO}$ were stimulated with anti-CD3 Ab and irradiated antigen-presenting cells (CD3-depleted splenocytes) plus IL-6 (20 ng/ml) and TGF-β (1 ng/ml). In some experiments, SOCS1-KIR (30 μM) or SOCS1-KIR2A (30 μM) was used for providing mimetic function of SOCS1. Cells were cultured for 4 days and then subjected to flow cytometric analysis.

Histology

Organs were removed from sacrificed mice, fixed in 10% neutral buffered formalin, embedded in paraffin, and sectioned for hematoxylin-eosin staining.

T-cell adoptive transfer

CD4$^+$CD25$^-$CD45RB^{hi} cells from the B6.SJL congenic mice (carrying the CD45.1 marker) and YFP$^+$ T_{reg} cells from WT or *Ube2n*$^{Treg\text{-}KO}$ mice were prepared by FACS sorting. *Rag1*$^{-/-}$ mice were injected i.p. with 4×10^5 syngeneic CD4$^+$CD25$^-$CD45RB^{hi} T cells either alone or together with WT T_{reg} or *Ube2n* KO T_{reg} cells (2×10^5). Mice were observed daily, and any mice showing clinical signs of severe disease were sacrificed. In some experiments, mice were administered, via i.p. injection (in 100 μl final volume), with SOCS1-KIR (60 μg/mouse), SOCS1-KIR2A (60 μg/mouse), or PBS every other day.

IB

Purified T_{reg} and CD4$^+$ T cells were lysed in RIPA buffer with proteasome inhibitors. The cell lysates were fractionated by SDS-PAGE and subjected to IB with the indicated antibodies.

Real-time quantitative RT-PCR

RNA isolation and real-time quantitative RT-PCR were performed as previously described[45]. The gene-specific primer sets are listed in Supplementary Table 1.

Luciferase reporter assay

Murine EL-4 T cells (2×10^5) were transfected, using lipofectamine (Invitrogen), with *Socs1*-Luc or *Socs1* mut-luc together with a control Renilla luciferase reporter. In some experiments, the cells were also cotransfected with the indicated cDNA expression vectors. After 30–40 h, the cells were either not treated or stimulated as indicated and subjected to dual luciferase assay (Promega). Specific luciferase activity was normalized based on the internal control Renilla luciferase activity in each sample.

ELISA

Immuno Plate Maxisorp plates (NUNC) were coated with 1μg/ml capture Abs for the indicated cytokines in 50 mM sodium bicarbonate and incubated overnight at 4°C. After blocking with 1% BSA in PBS, the plates were incubated with serially diluted standard or samples and then with HRP-conjugated detection antibodies. Following colorimetric reaction (tetramethylbnzidine; Moss), the absorbance at 450 nm was measured using an ELISA plate reader.

Statistical analysis

Prism software was used for two-tailed unpaired *t*-tests. *P* values of less than 0.05 or 0.01 were considered significant and very significant, respectively.

Supplementary Material

Refer to Web version on PubMed Central for supplementary material.

ACKNOWLEDGEMENTS

We thank Drs. M. Karin and T. Kishimoto for reagents. We also thank the personnel from the flow cytometry, the DNA analysis, and the histology core facilities at MD Anderson Cancer Center for technical assistance. This study was supported by grants from National Institutes of Health (AI057555, AI064639, GM84459) and the G. S. Hogan Gastrointestinal Cancer Research Fund.

REFERENCES

1. Sakaguchi S, Yamaguchi T, Nomura T, Ono M. Regulatory T cells and immune tolerance. Cell. 2008; 133:775–787. [PubMed: 18510923]
2. Rudensky AY. Regulatory T cells and Foxp3. Immunol. Rev. 2011; 241:260–268. [PubMed: 21488902]
3. Shevach EM. Mechanisms of foxp3+ T regulatory cell-mediated suppression. Immunity. 2009; 30:636–645. [PubMed: 19464986]
4. Rubtsov YP, et al. Stability of the regulatory T cell lineage in vivo. Science. 2010; 329:1667–1671. [PubMed: 20929851]
5. Bailey-Bucktrout SL, Bluestone JA. Regulatory T cells: stability revisited. Trends Immunol. 2011; 32:301–306. [PubMed: 21620768]
6. Hori S. Regulatory T cell plasticity: beyond the controversies. Trends Immunol. 2011; 32:295–300. [PubMed: 21636323]
7. Yang XO, et al. Molecular antagonism and plasticity of regulatory and inflammatory T cell programs. Immunity. 2008; 29:44–56. [PubMed: 18585065]
8. Duarte JH, Zelenay S, Bergman ML, Martins AC, Demengeot J. Natural T_{reg} cells spontaneously differentiate into pathogenic helper cells in lymphopenic conditions. Eur. J. Immunol. 2009; 39:948–955. [PubMed: 19291701]
9. Tsuji M, et al. Preferential generation of follicular B helper T cells from Foxp3+ T cells in gut Peyer's patches. Science. 323:1488–1492. (323). [PubMed: 19286559]
10. Zhou X, et al. Instability of the transcription factor Foxp3 leads to the generation of pathogenic memory T cells in vivo. Nat. Immunol. 2009; 10:1000–1007. [PubMed: 19633673]
11. Ayyoub M, et al. Human memory FOXP3+ T_{reg}s secrete IL-17 ex vivo and constitutively express the T(H)17 lineage-specific transcription factor RORgamma t. Proc. Natl. Acad. Sci. USA. 2009; 106:8635–8640. [PubMed: 19439651]
12. Voo KS, et al. Identification of IL-17-producing FOXP3+ regulatory T cells in humans. Proc. Natl. Acad. Sci. USA. 2009; 106:4793–4798. [PubMed: 19273860]
13. Takahashi R, et al. SOCS1 is essential for regulatory T cell functions by preventing loss of Foxp3 expression as well as IFN-{gamma} and IL-17A production. J. Exp. Med. 2011; 208:2055–2067. [PubMed: 21893603]
14. Xu L, Kitani A, Fuss I, Strober W. Cutting edge: regulatory T cells induce CD4+CD25-Foxp3- T cells or are self-induced to become T_H17 cells in the absence of exogenous TGF-beta. J. Immunol. 2007; 178:6725–6729. [PubMed: 17513718]
15. Collins EL, et al. Inhibition of SOCS1−/− lethal autoinflammatory disease correlated to enhanced peripheral Foxp3+ regulatory T cell homeostasis. J. Immunol. 2011; 187:2666–2676. [PubMed: 21788442]

16. Sakaguchi S. Naturally arising CD4+ regulatory T cells for immunologic self-tolerance and negative control of immune responses. Annu. Rev. Immunol. 2004; 22:531–562. [PubMed: 15032588]
17. Bhoj VG, Chen ZJ. Ubiquitylation in innate and adaptive immunity. Nature. 2009; 458:430–437. [PubMed: 19325622]
18. Sun L, Deng L, Ea C-K, Xia Z-P, Chen ZJ. The TRAF6 ubiquitin ligase and TAK1 kinase mediate IKK activation by BCL10 and MALT1 in T lymphocytes. Mol. Cell. 2004; 14:289–301. [PubMed: 15125833]
19. Yamamoto M, et al. Cutting Edge: Pivotal function of Ubc13 in thymocyte TCR signaling. J. Immunol. 2006; 177:7520–7524. [PubMed: 17114420]
20. Isomura I, et al. c-Rel is required for the development of thymic Foxp3+ CD4 regulatory T cells. J. Exp. Med. 2009; 206:3001–3014. [PubMed: 19995950]
21. Long M, Park SG, Strickland I, Hayden MS, Ghosh S. Nuclear factor-kappaB modulates regulatory T cell development by directly regulating expression of Foxp3 transcription factor. Immunity. 2009; 31:921–931. [PubMed: 20064449]
22. Ruan Q, et al. Development of Foxp3(+) regulatory t cells is driven by the c-Rel enhanceosome. Immunity. 2009; 31:932–940. [PubMed: 20064450]
23. Zheng Y, et al. Role of conserved non-coding DNA elements in the Foxp3 gene in regulatory T-cell fate. Nature. 2010; 463:808–812. [PubMed: 20072126]
24. Yamamoto M, et al. Key function for the Ubc13 E2 ubiquitin-conjugating enzyme in immune receptor signaling. Nat. Immunol. 2006; 7:962–970. [PubMed: 16862162]
25. Zhou X, et al. Selective miRNA disruption in T reg cells leads to uncontrolled autoimmunity. J. Exp. Med. 2008; 205:1983–1991. [PubMed: 18725525]
26. Srinivas S, et al. Cre reporter strains produced by targeted insertion of EYFP and ECFP into the ROSA26 locus. BMC Dev. Biol. 2001; 1:4. [PubMed: 11299042]
27. Morrissey PJ, Charrier K, Braddy S, Liggitt D, Watson JD. CD4+ T cells that express high levels of CD45RB induce wasting disease when transferred into congenic severe combined immunodeficient mice. Disease development is prevented by cotransfer of purified CD4+ T cells. J. Exp. Med. 1993; 178:237–244. [PubMed: 8100269]
28. Mattioli I, et al. Transient and selective NF-kappa B p65 serine 536 phosphorylation induced by T cell costimulation is mediated by I kappa B kinase beta and controls the kinetics of p65 nuclear import. J. Immunol. 2004; 172:6336–6344. [PubMed: 15128824]
29. Sasaki Y, et al. Canonical NF-kappaB activity, dispensable for B cell development, replaces BAFF-receptor signals and promotes B cell proliferation upon activation. Immunity. 2006; 24:729–739. [PubMed: 16782029]
30. Pasparakis M, et al. TNF-mediated inflammatory skin disease in mice with epidermis-specific deletion of IKK2. Nature. 2002; 417:861–866. [PubMed: 12075355]
31. Rubtsov YP, et al. Regulatory T cell-derived interleukin-10 limits inflammation at environmental interfaces. Immunity. 2008; 28:546–558. [PubMed: 18387831]
32. Chaudhry A, et al. Interleukin-10 signaling in regulatory T cells is required for suppression of T_H17 cell-mediated inflammation. Immunity. 2011; 34:566–578. [PubMed: 21511185]
33. Huber S, et al. T_H17 cells express interleukin-10 receptor and are controlled by $Foxp3^-$ and Foxp3+ regulatory CD4+ T cells in an interleukin-10-dependent manner. Immunity. 2011; 34:554–565. [PubMed: 21511184]
34. Pillemer BB, Xu H, Oriss TB, Qi Z, Ray A. Deficient SOCS3 expression in CD4+CD25+FoxP3+ regulatory T cells and SOCS3-mediated suppression of T_{reg} function. Eur. J. Immunol. 2007; 37:2082–2089. [PubMed: 17621372]
35. Cao S, Zhang X, Edwards JP, Mosser DM. NF-kappaB1 (p50) homodimers differentially regulate pro- and anti-inflammatory cytokines in macrophages. J. Biol. Chem. 2006; 281:26041–26050. [PubMed: 16835236]
36. Benkhart EM, Siedlar M, Wedel A, Werner T, Ziegler-Heitbrock HW. Role of Stat3 in lipopolysaccharide-induced IL-10 gene expression. J. Immunol. 2000; 165:1612–1617. [PubMed: 10903771]

37. Saito H, et al. IFN regulatory factor-1-mediated transcriptional activation of mouse STAT-induced STAT inhibitor-1 gene promoter by IFN-gamma. J Immunol. 2000; 164:5833–5843. [PubMed: 10820262]

38. Diehl S, et al. Inhibition of T_H1 differentiation by IL-6 is mediated by SOCS1. Immunity. 2000; 13:805–815. [PubMed: 11163196]

39. Charoenthongtrakul S, Zhou Q, Shembade N, Harhaj NS, Harhaj EW. Human T cell leukemia virus type 1 Tax inhibits innate antiviral signaling via NF-kappaB-dependent induction of SOCS1. J. Virol. 2011; 85:6955–6962. [PubMed: 21593151]

40. Flowers LO, et al. Characterization of a peptide inhibitor of Janus kinase 2 that mimics suppressor of cytokine signaling 1 function. J. Immunol. 2004; 172:7510–7518. [PubMed: 15187130]

41. Flowers LO, Subramaniam PS, Johnson HM. A SOCS-1 peptide mimetic inhibits both constitutive and IL-6 induced activation of STAT3 in prostate cancer cells. Oncogene. 2005; 24:2114–2120. [PubMed: 15688010]

42. Jager LD, et al. The kinase inhibitory region of SOCS-1 is sufficient to inhibit T-helper 17 and other immune functions in experimental allergic encephalomyelitis. J. Neuroimmunol. 2011; 232:108–118. [PubMed: 21131060]

43. Kryczek I, et al. IL-17+ regulatory T cells in the microenvironments of chronic inflammation and cancer. J. Immunol. 2011; 186:4388–4395. [PubMed: 21357259]

44. Harhaj EW, Maggirwar SB, Sun S-C. Inhibition of p105 processing by NF-κB proteins in transiently transfected cells. Oncogene. 1996; 12:2385–2392. [PubMed: 8649779]

45. Chang M, et al. The ubiquitin ligase Peli1 negatively regulates T cell activation and prevents autoimmunity. Nat. Immunol. 2011; 12:1002–1009. [PubMed: 21874024]

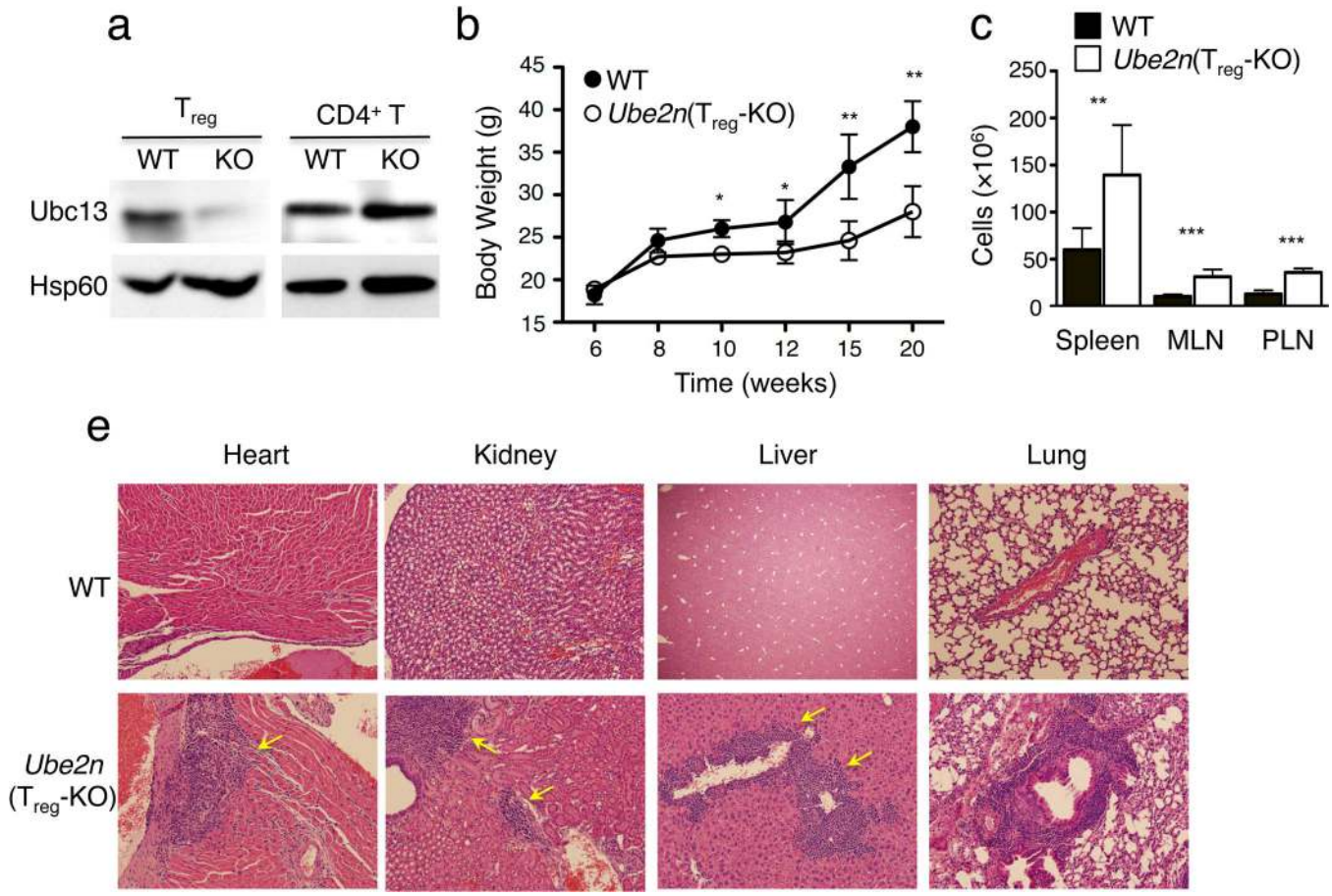

Figure 1. T_{reg}-specific ablation of Ubc13 causes systemic autoimmunity

(**a**) immunoblot of Ubc13 expression in $CD4^+$ T cells and T_{reg} cells sorted from *Ube2n*$^{fl/fl}$Foxp3$^{GFP\text{-}Cre}$ (KO) and *Ube2n*$^{+/+}$Foxp3$^{GFP\text{-}Cre}$ (WT) mice. Loading control: protein Hsp60. Data are representative of two independent experiments. (**b**) Bodyweight of *Ube2n*$^{Treg\text{-}KO}$ and *Ube2n*$^{+/+}$Foxp3$^{GFP\text{-}Cre}$ (WT) measured at the indicated times and presented as mean±SD. Results were from a total of three independent experiments (5–7 mice/genotype in each experiment). *p=0.05; **p=0.01 (two-tailed unpaired t-test). (**c**) Number of total cells from spleen, mesenteric lymph node (MLN) and peripheral lymph node (PLN) of age- and sex-matched *Ube2n*$^{Treg\text{-}KO}$ and *Ube2n*$^{+/+}$Foxp3$^{GFP\text{-}Cre}$ (WT) 10 week old mice presented as the mean±SD value. **p=0.01 and ***p=0.001 (two-tailed unpaired t-test). Data are representative of two independent experiments. (**d**) H&E staining of various non-lymphoid tissue sections from 20 weeks old *Ube2n*$^{Treg\text{-}KO}$ and *Ube2n*$^{+/+}$Foxp3$^{GFP\text{-}Cre}$ (WT) mice. Data are representative of 3–4 mice/genotype.

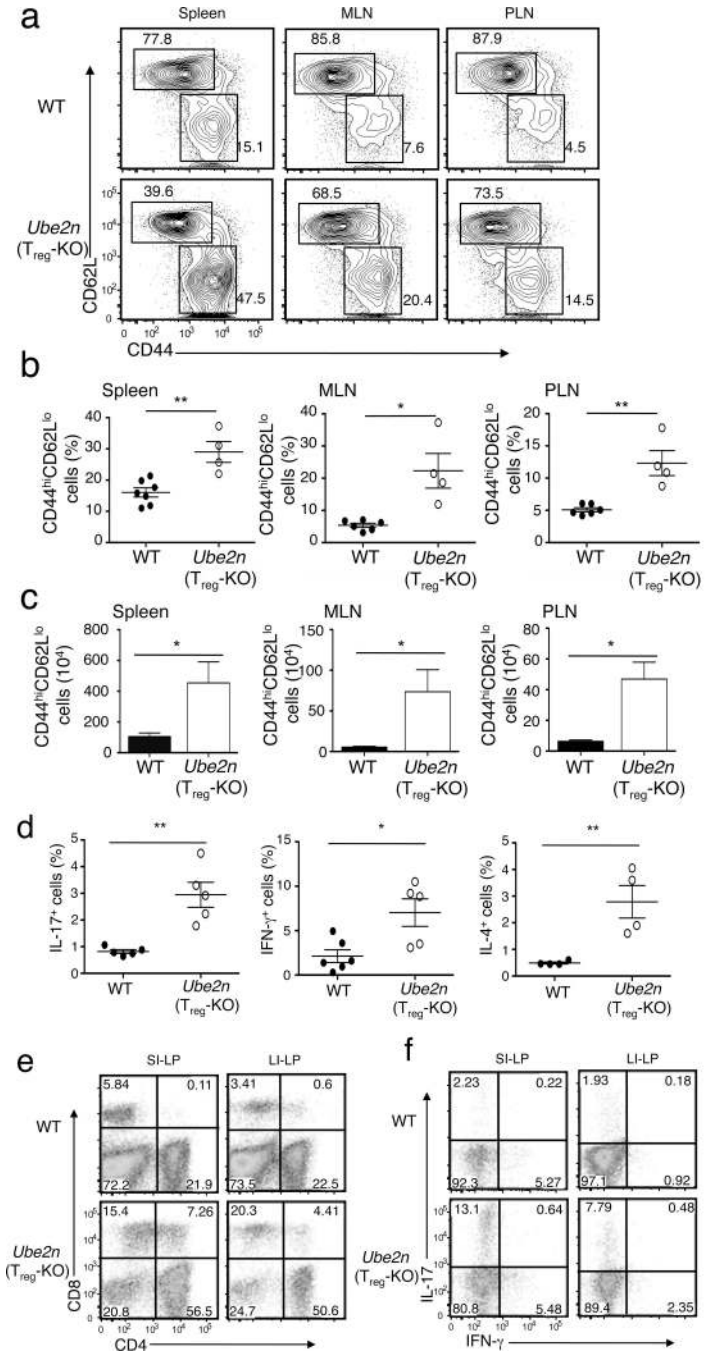

Figure 2. T_{reg}-specific ablation of Ubc13 impairs T-cell homeostasis

(**a**) Flow cytometric analysis of T cells derived from the indicated lymphoid organs of WT and *Ube2n*$^{Treg\text{-}KO}$ mice (8 weeks old), showing the percentage of naïve ($CD44^{lo}CD62L^{hi}$) and memory-like ($CD44^{hi}CD62L^{lo}$) $CD4^+$ T cells. Data are representative of five experiments with three mice per group. (**b, c**) Summary (mean ± SD value) of the frequency (**b**) and absolute numbers (**c**) of memory-like $CD4^+$ T cells in the indicated lymphoid organs of WT and *Ube2n*$^{Treg\text{-}KO}$ mice (8 weeks old), determined by flow cytometry. *p=0.05 and **p=0.01 (two-tailed unpaired t-test). (**d**) ICS measuring the frequency of IL-17-, IFN-γ,

and IL-4-producing $CD4^+$ T cells (gated on $CD3^+CD4^+$ cells) within the spleen of WT and *Ube2n*$^{Treg\text{-}KO}$ mice (8–10 weeks old). *p=0.05 and **p=0.01 (two-tailed unpaired t-test). Data are representative of three independent experiments (each circle represents one mouse). (**e, f**) Flow cytometric analyses of $CD4^+$ or $CD8^+$ (**e**) and IL-17- and IFN-γ-producing $CD4^+$ T cells (**f**) from small intestine lamina propria (SI-LP) and large intestine lamina propria (LI-LP) of WT and *Ube2n*$^{Treg\text{-}KO}$ mice (8 weeks old). Numbers in quadrants indicate percentage of cells. Data are representative of two experiments with three mice per group.

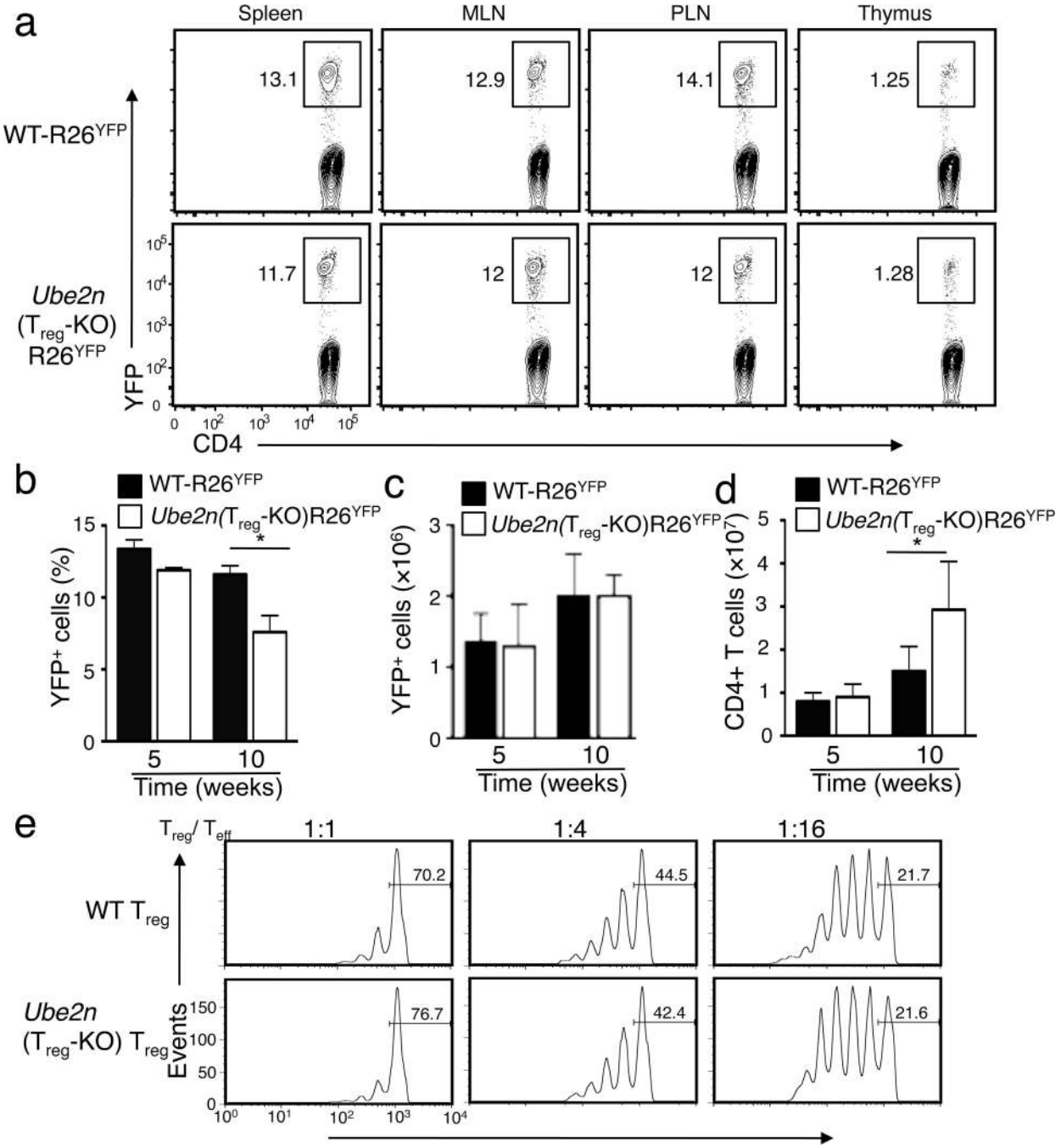

Figure 3. Ubc13 is dispensable for T_{reg} homeostasis and *in vitro* suppressive activity

(**a**) Flow cytometric analysis of the frequency of YFP^+ T_{reg} cells (among $CD3^+CD4^+$ cells) in the indicated lymphoid organs of 6 weeks old mice. Data are representative of five experiments with three mice per group. (**b–d**) Frequency (**b**) and absolute number (**c**) of YFP^+ cells (among $CD3^+CD4^+$ cells) and absolute number of total $CD4^+$ T cells (d) in the spleen of the indicated ages of mice, measured by flow cytometry and shown as the mean ±SD value. *p=0.05 (n=5) (two-tailed unpaired t-test). (**e**) *In vitro* suppressive activity of T_{reg} cells, measured based on the proliferation (CFSE dilution) of naïve $CD4^+$ T cells

activated by anti-CD3 plus antigen-presenting cells (irradiated CD3-depleted splenocytes from WT mice) in the presence of the indicated ratios of sorted T_{reg} cells derived from WT or *Ube2n*$^{Treg\text{-}KO}$ mice (6 weeks old). The percentage of undivided cells is indicated.

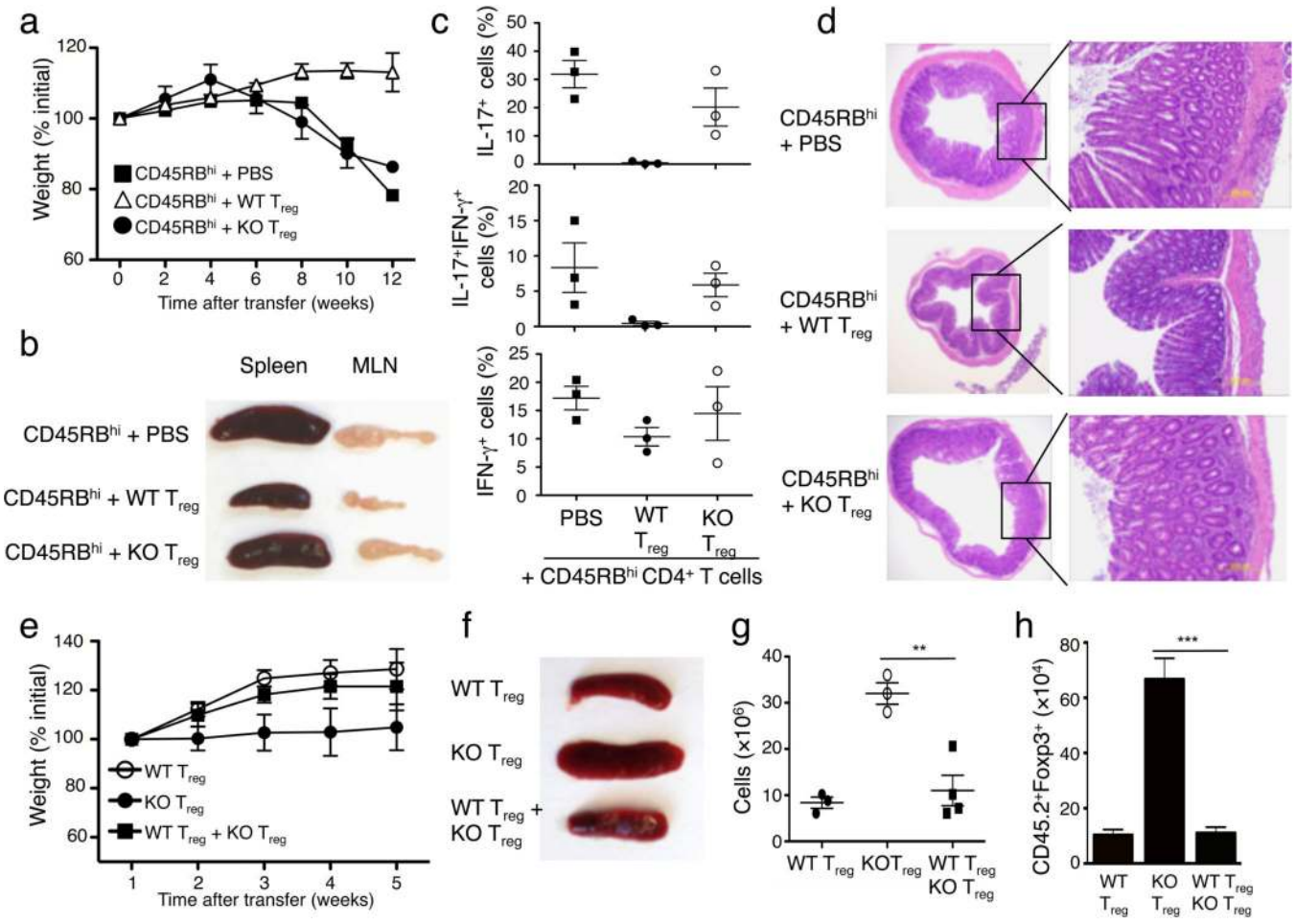

Figure 4. T_{reg}-specific Ubc13 ablation impairs the *in vivo* immunosuppressive function of T_{reg} cells

(**a–d**) Disease phenotypes of *Rag1* KO mice (6 weeks old) adoptively transferred with WT CD45.1$^+$ congenic CD45RB^{hi} naïve CD4$^+$ T cells together with either PBS or sorted T_{reg} cells derived from WT or *Ube2n*$^{Treg\text{-}KO}$ mice (6 weeks old). Bodyweight was measured at the indicated times and presented as percentage of initial weight (mean±SD) (**a**). A representative lymphoid organ picture (**b**), frequency of the indicated cytokine-producing effector CD4$^+$ T cells in the MLN (measured by flow cytometry and gated on CD45.1$^+$ cells) (**c**), and H&E staining of colon (**d**) were obtained from recipient mice at 12 weeks after adoptive transfer. Data are from a total of three independent experiments (3 recipient mice per group in each experiment). (**e–h**) Disease phenotypes of *Rag1* KO mice (5 weeks old) adoptively transferred with CD45.1$^+$Foxp3$^+$ WT T_{reg} (from B6.SJL congenic mice) and/or CD45.2$^+$Foxp3$^+$ *Ube2n*$^{Treg\text{-}KO}$ (KO) T_{reg} cells. Bodyweight was measured weekly after transfer (**e**). A representative picture of spleen (**f**), absolute number of total splenocytes (**g**, presented as mean±SD value), and absolute number of CD45.2$^+$Foxp3$^+$ cells from the spleen (**h**, presented as the mean±SD value) were determined 5 weeks after transfer. **p=0.01 (two-tailed unpaired t-test).

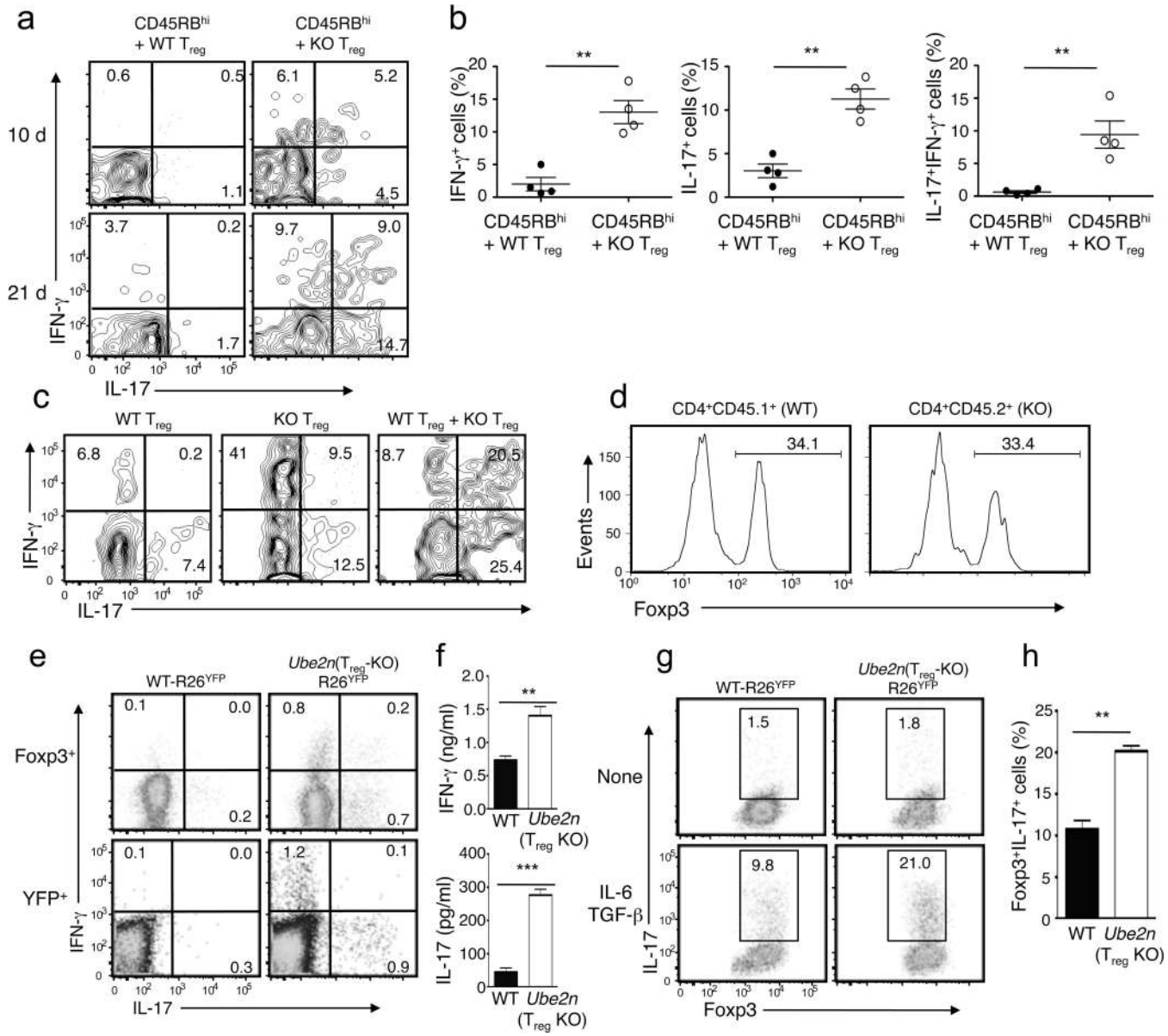

Figure 5. Ubc13-deficient T_{reg} cells are sensitive to lymphopenic and inflammatory conditions for acquiring effector functions

(**a, b**) Flow cytometry analysis of IL-17- and IFN-γ-producing MLN T_{reg} cells (gated on CD45.2$^+$Foxp3$^+$CD4$^+$ cells) derived from *Rag1* KO mice (6 weeks old) adoptively transferred, for 10 or 21 days, with WT CD45.1$^+$CD4$^+$CD25$^-$CD45RB^{hi} T cells plus CD4$^+$YFP$^+$ T_{reg} cells purified from WT-R26^{YFP} (WT) or *Ube2n*$^{Treg\text{-}KO}$R26^{YFP} (KO) mice (6 weeks old, CD45.2$^+$). Data are representative (**a**) or summary (**b**, day 21 data only) of two independent experiments (n=3). *p=0.05. (**c**) Flow cytometry analysis of IL-17- and IFN-γ-producing MLN T_{reg} cells (gated on CD45.2$^+$Foxp3$^+$ cells) from *Rag1* KO mice (5 weeks old) adoptively transferred, for 5 weeks, with CD45.1$^+$Foxp3$^+$ WT and/or CD45.2$^+$Foxp3$^+$ *Ube2n*$^{Treg\text{-}KO}$ (KO) T_{reg} cells. (**d**) Flow cytometric analysis of Foxp3 expression in CD45.1$^+$Foxp3$^+$ and CD45.2$^+$Foxp3$^+$ T_{reg} cells from the *Rag1 KO* recipients of WT plus

KO T_{reg} cells described in **d**. (**e**) Flow cytometry measuring the frequency of IL-17- and IFN-γ-expressing T_{reg} cells in the spleen of 10 weeks old mice, gating on $Foxp3^+$ or YFP^+ cells. (**f**) ELISA quantifying the secreted IFN-γ and IL-17 by YFP^+CD4^+ T_{reg} cells (isolated from 10 weeks old mice), stimulated with PMA and ionomycin for 24 h. Data are presented as means±SD of two independent experiments. (**g, h**) Flow cytometric analysis of the frequency of $Foxp3^+IL\text{-}17^+$ cells in sorted YFP^+CD4^+ T_{reg} cells, derived from the indicated mice (6 weeks old) and activated in the absence or presence of TGF-β and IL-6. Data are representative (**e**) or summary (**f**) of four independent experiments (n=3). **p=0.01.

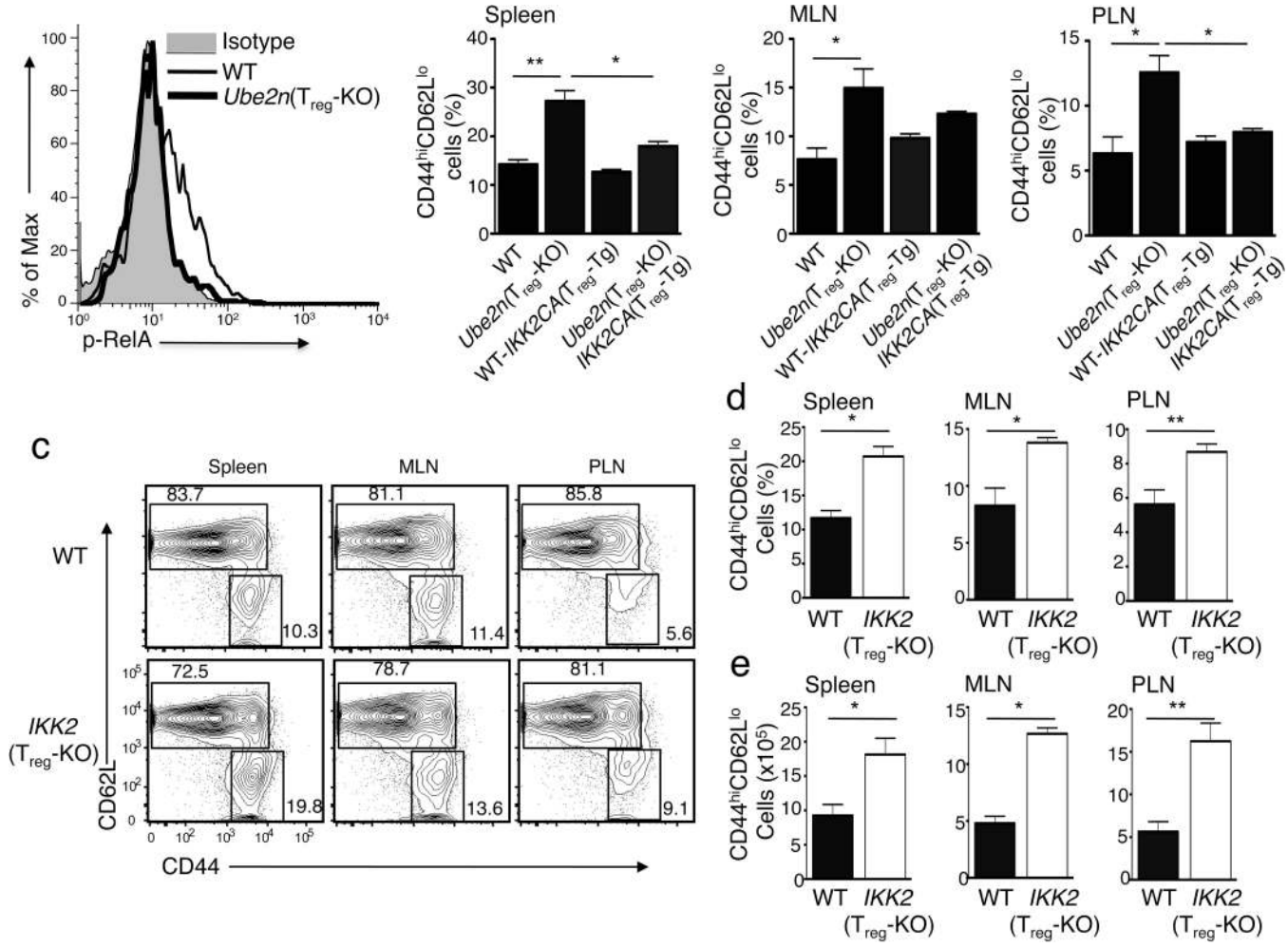

Figure 6. The T_{reg}-specific function of Ubc13 involves its downstream target IKK

(**a**) Flow cytometric analysis of RelA phosphorylation in sorted T_{reg} cells from WT or *Ube2n*$^{Treg\text{-}KO}$ mice, stimulated with anti-CD3 and anti-CD28 for 15 min using a crosslinking method[45]. (**b**) Flow cytometric analysis of CD44^{hi}CD62L^{lo} memory-like T cells (gated on CD3^{+}CD4^{+} cells) within different lymphoid organs of the indicated mice (6–8 weeks old). Data are presented as mean ± SD value and representative of three independent experiments. *p=0.05 and **p=0.01 (two-tailed unpaired t-test). (**c**) Flow cytometric analysis of CD4^{+} T cells derived from the indicated lymphoid organs of WT or *IKK2*$^{Treg\text{-}KO}$ mice (7 weeks old), measuring the percentage (numbers in quadrangles) of naïve (CD44^{lo}CD62L^{hi}) and memory-like (CD44^{hi}CD62L^{lo}) T cells. Data are representative of three experiments. (**d, e**) Flow cytometric analysis of the frequency (**d**) and absolute number (**e**) of CD44^{hi}CD62^{lo} memory-like CD4^{+} T cells in the indicated lymphoid organs of WT and *IKK2*$^{Treg\text{-}KO}$ littermates (7 weeks old). Data are representative of two independent experiments.

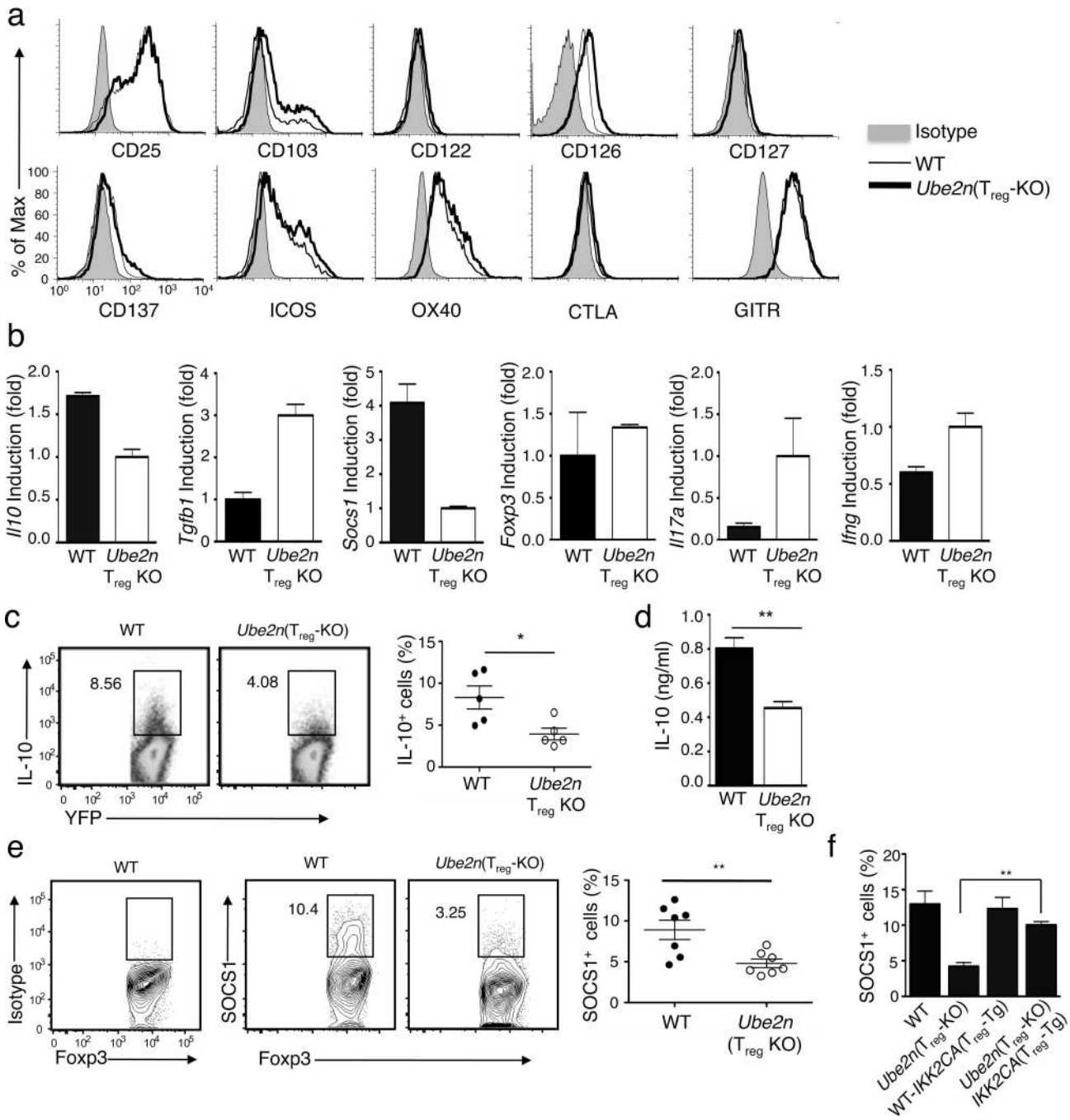

Figure 7. Ubc13 is dispensable for expression of T_{reg} signature genes but regulates expression SOCS1 and IL-10

(**a**) Flow cytometric analysis of splenocytes derived from WT-R26^{YFP} and *Ube2n*$^{Treg\text{-}KO}$R26^{YFP} mice (5 weeks old), measuring the expression of surface markers on T_{reg} cells (gated on Foxp3$^+$CD4$^+$). Data are representative of two independent experiments. (**b**) Real-time RT-PCR analysis of the relative mRNA expression level of the indicated genes in YFP$^+$CD4$^+$ T_{reg} cells, sorted (based on YFP) from 5-week old WT-R26^{YFP} and *Ube2n*$^{Treg\text{-}KO}$R26^{YFP} mice. Data were normalized to a reference gene, β-actin. (**c**) Flow

cytometry measuring the frequency of IL-10-producing cells among the YFP^+CD4^+ T_{reg} cells from MLN of WT-$R26^{YFP}$ and *Ube2n*$^{Treg\text{-}KO}R26^{YFP}$ mice (5 weeks old). Data are representative (left) and summary (right) of three independent experiments (n=5/genotype). *p=0.05 (two-tailed unpaired t-test). (**d**) ELISA determining IL-10 production by purified YFP^+CD4^+ T_{reg} cells stimulated with PMA and ionomycin for 24 h. Data are mean±SD of three independent experiments. (**e**) Flow cytometric analysis of SOCS1-expressing cells in $Foxp3^+CD4^+$ T_{reg} cells from MLN of WT-$R26^{YFP}$ and *Ube2n*$^{Treg\text{-}KO}R26^{YFP}$ mice (6 weeks old). Data are representative (left) and summary (right) of three independent experiments (n=4–7/genotype in each experiment). **p=0.01 (two-tailed unpaired t-test). (**f**) Flow cytometric analysis of SOCS1-expressing T_{reg} cells in the indicated littermates (6 weeks old), presented as a summary graph. **p=0.01 (two-tailed unpaired t-test).

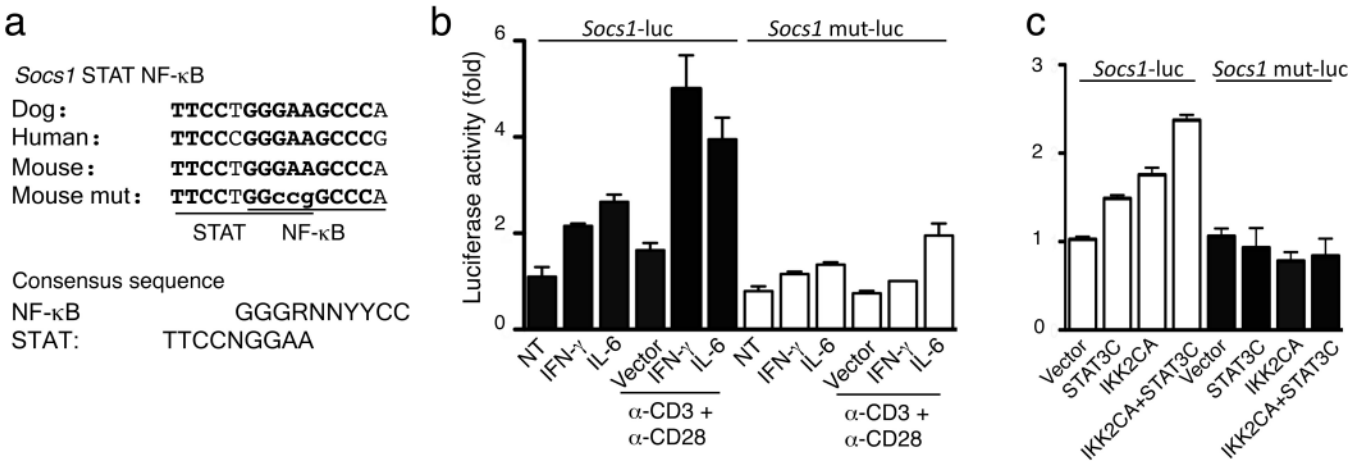

Figure 8. Synergistic activation of *Socs1* promoter by IKK2 and STAT3 via a STAT-NF-κB composite

(**a**) A putative NF-κB-binding sequence with an overlapping STAT-binding site. Mutated nucleotides in *Socs1* mut-luc are shown in lower-case letters. STAT- and NF-κB-binding consensus sites are shown below. (**b**) Luciferase assays determining the activation of *Socs1*-luciferase and *Socs1*-mut luciferase reporters in EL-4 cells stimulated by the indicated inducers. Luciferase activity was normalized to Renilla luciferase and presented as fold of induction compared to the non-treated (NT) cells. Data are representative of three independent experiments with consistent results. (**c**) Luciferase assays measuring the activation of *Socs1*-luciferase and *Socs1*-mut luciferase reporters in EL-4 cells by the constitutively active *STAT3* (*STAT3C*) and *IKK2* (*IKK2CA*). Luciferase activity was determined as in **b** and presented as fold of induction compared to the vector-transfected cells. Data are representative of three independent experiments with consistent results.

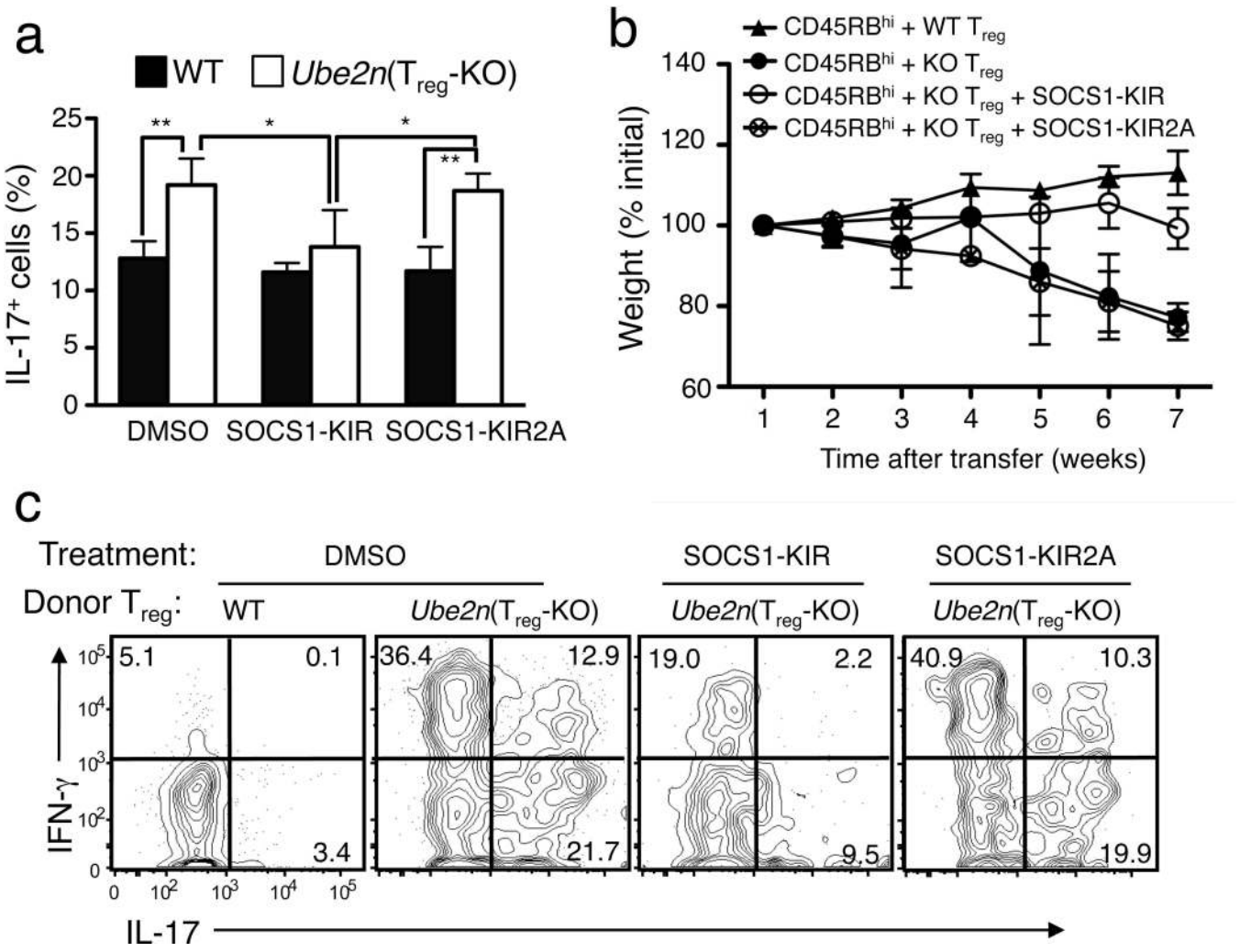

Figure 9. A SOCS1 mimetic peptide partially rescues the functional defect of Ubc13-deficient T_{reg} cells both *in vitro* and *in vivo*

(**a**) Flow cytometry measuring the frequency of IL-17-producting cells in sorted YFP$^+$CD4$^+$ T_{reg} cells derived from WT-R26^{YFP} and *Ube2n*$^{Treg\text{-}KO}$R26^{YFP} mice, activated under T_H17 polarizing conditions in the presence of DMSO, the SOCS1 mimetic peptide SOCS1-KIR, or the negative control peptide SOCS1-KIR2A. *p=0.05, **p=0.01 (two-tailed unpaired t-test). Data are representative of two independent experiments. (**b,c**) Disease phenotypes of *Rag1* KO mice (5 weeks old) adoptively transferred with WT CD45.1$^+$CD4$^+$CD25$^-$CD45RB^{hi} naïve T cells together with CD4$^+$YFP$^+$ T_{reg} cells purified from WT-R26^{YFP} or *Ube2n*$^{Treg\text{-}KO}$R26^{YFP} mice (6 weeks old). The recipient mice were either not treated or injected (i.p.) with SOCS1-KIR or SOCS1-KIR2A every other day. Bodyweight of recipient mice was measured at different times and presented as percentage of initial weight (**b**), and the frequency of IL-17$^+$ or IFN-γ$^+$ cells among the transferred CD4$^+$YFP$^+$ T_{reg} cells was determined by flow cytometry (gated on CD45.2$^+$ cells) after 7 weeks of transfer (**c**).